

Quantifying the Unseen: Epidemiological Underestimation Problem for COVID-19

M. Aykut Attar*

Ayça Tekin-Koru**

Abstract

Reliable epidemiological data is a prerequisite for meaningful economic analysis of pandemic-related policies, as it provides the foundation for evaluating public health measures and their economic impacts. In Türkiye, the government did not disclose the number of all confirmed COVID-19 cases for several months after the relaxation of initial mobility restrictions in June 2020, creating significant challenges for assessing the economic and health tradeoffs of these policies. This paper addresses this issue by developing a system dynamics approach that can identify and quantify epidemiological underestimation under extreme data limitations. Our simulation algorithm builds on a nonlinear dynamical model that explicitly accounts for individuals that are exposed but not yet infectious and requires only a few reliable data points. Results imply large deviations between official and estimated figures, and counterfactual experiments show that social distancing, if practiced well and long enough, would have been highly effective for the containment of COVID-19.

JEL Codes: C32, C63, I18

Keywords: nonlinear systems, SEIRD model, underreporting, social distancing

* *Corresponding author*, Dept. of Economics, FEAS, Hacettepe University, Beytepe Campus, 06800 Cankaya/Ankara, Türkiye, maattar@hacettepe.edu.tr, <https://orcid.org/0000-0003-0142-713X>

** Dept. of Economics, TED University, Ziya Gökalp Caddesi, No.47, 06420 Çankaya/Ankara, Türkiye, ayca.tekinkoru@tedu.edu.tr, <https://orcid.org/0000-0002-0817-9055>

Görünmeyi Ölçmek: COVID-19 için Epidemiyolojik Eksik Tahminleme Sorunu

Öz

Güvenilir epidemiyolojik veriler, pandemiyle ilişkili politikaların kamu sağlığı önlemleri ve ekonomik etkiler açısından anlamlı bir şekilde analiz edilebilmesi için zorunlu bir ön koşuldur. Türkiye’de hükümet, ilk hareket kısıtlamalarının Haziran 2020’de gevşetilmesinden sonraki aylar boyunca, teyit edilen tüm COVID-19 vakalarının sayısını açıklamamış ve bu durum, bu politikaların ekonomik ve sağlık ödünleşmelerinin değerlendirilmesini ciddi şekilde zorlaştırmıştır. Bu makale, aşırı veri sınırlılıkları altında bile epidemiyolojik eksik tahminlemeyi tespit edebilen ve nicel olarak değerlendirebilen bir sistem dinamiği yaklaşımı geliştirmektedir. Simülasyon algoritmamız, virüse maruz kalan fakat henüz bulaştırıcı olmayan bireyleri açıkça dikkate alan bir doğrusal olmayan dinamik model üzerinde inşa edilmekte ve sadece birkaç güvenilir veri noktasına sahip olunmasını gerektirmektedir. Bulgular, resmî ve tahmin ettiğimiz sayılar arasında büyük farklılaşmalara işaret etmekte, karşıolgusal deneyler sosyal mesafe politikalarının yeterince iyi biçimde ve yeterince uzun süre uygulandığında COVID-19’un kontrol altında tutulması için oldukça etkili olabileceğini göstermektedir.

JEL Kodları: C32, C63, I18

Anahtar sözcükler: doğrusal olmayan sistemler, SEIRD modeli, eksik raporlama, sosyal mesafe

1. Introduction

The COVID-19 pandemic led governments across the globe to impose mobility restrictions on people, also known as lockdown policies. The primary aim of these policies was to control the pandemic by reducing the speed of virus transmission through minimizing physical contact. However, these restrictions resulted in substantial contractions in real economic activity, impacting both supply and demand channels. By the first quarter of 2020, many countries experienced the largest economic downturns in recent history, underscoring the tradeoffs inherent in pandemic management strategies.

The earliest works by economists on the COVID-19 pandemic emphasized the necessity of evaluating the tradeoffs between economic and public health outcomes. Novel concepts such as the pandemic possibility frontier highlighted how fewer deaths could be achieved only under stricter mobility restrictions, which, in turn, imposed larger economic costs (e.g., Kaplan, Moll, & Violante, 2020). Yet, subsequent studies suggested that the relationship between economic and pandemic outcomes could be more nuanced. For instance, tighter and longer initial lockdowns might create a more stable public health environment for subsequent months, thus potentially mitigating long-term economic costs (e.g., Çakmaklı, Demiralp, Özcan, Yeşiltaş, & Yıldırım, 2023). Such insights gave rise to the “hammer and dance” framework, which identified the optimal strategy for managing the pandemic as one of imposing timely, stringent lockdowns (the hammer) and gradually relaxing them as the situation improved (the dance) (Hellwig, Assenza, Collard, Dupaigne, Feve, Kankanamge, & Werquin, 2022).

Central to all these analyses is the assumption of reliable epidemiological data. However, significant underestimation—arising from either unintentional gaps in testing or intentional data manipulation—challenges this foundation, leaving economic analyses vulnerable to inaccuracies. This article addresses this critical gap by presenting a system dynamics approach that identifies and quantifies epidemiological underestimation, offering a robust tool to ensure that economic analyses are grounded in reliable data. By focusing on Türkiye’s experience during the COVID-19 pandemic, the study provides broader insights into how such underestimation can be addressed in contexts of extreme data limitations.

Epidemiological underestimation, as demonstrated in the case of Türkiye, poses substantial challenges for accurately managing public health crises and evaluating their economic consequences. Successful management of a pandemic in any case necessitates the availability of reliable estimates of epidemiological variables such as daily infection rates and cumulative case counts. The challenge in this respect is *epidemiological underestimation*. As recently classified by Millimet and Parmeter (2022), epidemiological underestimation has two general types, (i) *under-ascertainment* problems that are mainly due to poor performance

in testing and surveillance, and (ii) *underreporting* problems that have unintentional and/or intentional causes. Unintentional underreporting is associated with misdiagnosis of individuals that recover or die without diagnosed with the disease. Intentional underreporting, on the other hand, is a result of corrupt data disclosure practices pursued for the legitimization of certain economic policies and public health measures.

Starting from the very early days of the COVID-19 pandemic, there has been a growing literature on epidemiological underestimation (e.g., Dougherty, Smith, Carson, & Ogden, 2021; Ghaffarzagdegan & Rahmandad, 2020; Giordano et al., 2020; Korolev, 2021; Krantz & Srinivasa Rao, 2020; Millimet & Parmeter, 2022; Rahmandad, Lim, & Sterman, 2021; Sawano et al., 2020; Wu et al., 2020). Several studies have demonstrated the extent of underestimation for COVID-19 by documenting the weekly excess deaths observed during the pandemic relative to the death counts of earlier years (e.g., Karlinsky & Kobak, 2021; Kung et al., 2021; Vadoros, 2020). Another group of studies has used forensic methods such as the Benford (1938) Law to investigate whether governments misreport COVID-19 statistics (e.g., Adıgüzel, Cansunar, & Çörekçioğlu, 2020; Balashov, Yan, & Zhu, 2020; Isea, 2020; Kapoor, Malani, Ravi, & Agrawal, 2020).² Finally, some studies have explored epidemiological underestimation by constructing compartmental epidemiology models *à la* Kermack and McKendrick (1927) and estimating these models with classical and Bayesian techniques as well as simulation-based algorithms (e.g., Çakmaklı & Şimşek, 2021; Chudik, Pesaran, & Rebucci, 2021; Ghaffarzagdegan & Rahmandad, 2020; Korolev, 2021; Millimet & Parmeter, 2022; Rahmandad, Lim, & Sterman, 2021). Clearly, the first two groups of studies build on *ex post* methodologies and cannot identify the actual epidemiological structure that features nonlinear dynamics and reinforcing and/or balancing feedback loops.

In this paper, we develop a system dynamics approach to detect the existence and severity of underestimation in the case of COVID-19 *under extreme data limitations*. As in the third group of studies mentioned above, we use a compartmental epidemiology model to accurately capture the actual progression of the pandemic in time. Specifically, we extend the Susceptible-Exposed-Infectious-Recovered-Deceased (SEIRD) model with underestimation and time-varying social distancing.³ As we discuss below in detail, we keep the model intentionally simple since we develop our simulation algorithm to work with only a few reliable data points and without any reliable data on key variables such as hospitalizations and intubated patients. Specifically, our model has only one reinforcing feedback loop (i.e.,

² The Benford Law states that, in many of the naturally-occurring groups of numbers, the first digit is not uniformly distributed and is expected to be small. Large deviations from the theoretical Benford distribution are therefore interpreted as manipulated or fraudulent data.

³ Many papers in the related literature work with SIR or SIRD versions, but the virus causing COVID-19 has a strictly positive incubation period. Hence, one needs to explicitly account for the number of *individuals that are infected but not yet infectious*.

contagion) and two exogenous driving forces (i.e., social distancing and underestimation). Using Google's mobility data for time-varying social distancing and fixing some of the disease-specific parameters at the outset, we calibrate the country-specific parameters of the model in a rigorous manner. Building on these, we estimate the total numbers of cases and deaths and then compare them with official statistics. Our system dynamics approach naturally lends itself to investigate the effects of social distancing on cases and deaths using counterfactual experiments as well.

Our methodological contribution to the literature on epidemiological underestimation is that the model-based algorithm we develop works when official statistics are almost completely unreliable. That is, we are able to estimate the actual headcounts of cases and deaths for the COVID-19 pandemic only with a few reliable data points. The problematic second wave of the pandemic in Türkiye, as we discuss below in detail, requires exactly this type of algorithm since the Turkish government did not disclose the number of all confirmed COVID-19 cases for several months. Clearly, with appropriate modifications, our algorithm can be applied to any other country and any other epidemic disease.

Our results for Türkiye show that the actual cumulative death count may be as large as 27,437 deaths by December 10th, 2020 for which the official cumulative death count is 15,571. We also estimate that, from the second week of June 2020 to the last week of November 2020, the total number of confirmed cases remains considerably larger than the official figures. At its highest, the difference is around 1 million people in late November. Our counterfactual analyses indicate that a later relaxation of mobility restrictions in the beginning of July would imply around 3,500 fewer deaths by December 10th, 2020. Finally, we show that the total death count by this date would be as low as 10,373 if social distancing was sustained at its historical maximum observed in the last week of April 2020 during the initial lockdown.

2. Background and Motivation

In epidemiology, underestimation of cases and deaths is a serious challenge (Gibbons et al., 2014; Noufaily, 2019). Epidemiologists try to determine the size of epidemic risks to inform policymakers once a disease outbreak occurs. Social scientists from various disciplines aim to understand demographic, economic, political, and social consequences of an epidemic or a pandemic. Governments need to develop appropriate policies to control the spread of the disease and minimize the costs associated with it.

Underestimation is more likely to occur in the initial stages of an extreme event such as the COVID-19 pandemic. The standard procedures in regards to first response,

mobilization of resources, and data disclosure practices develop as people and governments build experience around the event. It is almost unavoidable to have underestimation due to under-ascertainment and unintentional underreporting during the first weeks and months following the first exposure to the event. However, these types of unintentional underestimation may continue in the medium and long run only when state capacity is low and/or the government has an incentive to misreport epidemiological statistics. Therefore, in worldwide health crises, one would expect underestimation in almost any country in the initial stages, but it continues only in countries that lack the resources and/or incentives to correctly measure and report the statistics.

The Turkish government responded to the COVID-19 pandemic with several non-pharmaceutical interventions (NPIs) after the first case in Türkiye was confirmed on March 10th, 2020. The initial set of NPIs in Türkiye included (i) age-dependent curfews, (ii) workplace and school closures, (iii) the cancellation of social events and gatherings, and (iv) limitations on public transportation. These policy measures decreased interpersonal contact in public places via social distancing. As a result, the total number of confirmed cases exhibited a decreasing growth trend after the end of April 2020. Mobility restrictions were relaxed in June 2020 presumably because of severe economic costs of NPIs.

From the first days of the pandemic to late July 2020, the Turkish government reported daily numbers of tests, cases, and deaths along with recovered individuals in a now-famous *Turquoise Table* every night on TV screens. On July 29th, 2020, however, a “regime switch” happened in terms of the metrics reported in this table: The government abandoned reporting cases that tested positive for COVID-19 and started reporting metrics related to the so-called “patients,” i.e., the cases with moderate or severe symptoms only. After that, an alarming increase in the number of deaths in excess of previous years’ averages has surfaced in data from different official sources, contradicting the official COVID-19 death statistics.⁴ This misreporting practice was later admitted by government officials, and it ended on November 25th, 2020. Still, there was no correction in the official statistics for previous months.

The end result in the Turkish case is a sufficiently long period for which official COVID-19 statistics are completely unreliable. In such a case, likelihood-based inference using classical or Bayesian techniques requires the econometrician to correctly specify the data generating processes for measurement errors. That is, estimates necessarily depend on whether the structural model correctly specifies potentially time-varying and perhaps erratic patterns of underestimation.

⁴ Güçlü Yaman’s excess death statistics for Türkiye, based on different official resources, can be accessed at <https://github.com/gucluyaman/Excess-mortality-in-Turkey>.

The alternative we propose in this paper does not require us to specify the data generating processes for measurement errors; we take epidemiological underestimation as an exogenous and unobserved driving force affecting only the official counts, not the actual ones. Hence, instead of attempting an econometric estimation with measurement errors, we develop and implement a simulation-based algorithm that exploits the SEIRD model in an efficient and effective way. With only one observed country-specific mobility variable and two (daily) epidemiological data moments that are reliable, our algorithm takes only a few minutes to *jointly and exactly identify* two country-specific structural parameters.

Extreme data limitations in the Turkish case also motivate a sufficiently simple model. For the first and second waves of the pandemic in Türkiye, we do not have daily data on hospitalizations, intubated patients, intensive care occupancy rate, vaccinations, and other key health variables. For this reason, we construct a SEIRD model where contagion is the only decisive feedback loop.

3. Model

In this section, we introduce and analyze a version of the SEIRD model extended with time-varying social distancing. The SEIRD model is a dynamical, epidemiological model that divides population into different disease *compartments* (or *states*) on any particular day. These compartments are those of Susceptible (S), Exposed (E), Infectious (I), Recovered (R), and Deceased (D) individuals. The model determines how the fraction of people in different compartments change from one day to the next.

Consider the deterministic version of the SEIRD model studied by Degue and Le Ny (2018) and extended with a social distancing term as in Attar and Tekin-Koru (2022). The laws of motion are specified by the following set of (coupled) nonlinear difference equations:

$$S_{t+1} = S_t - \bar{\beta}\zeta(1 - d_t)^2 S_t I_t \quad (1)$$

$$E_{t+1} = E_t + \bar{\beta}\zeta(1 - d_t)^2 S_t I_t - \bar{\alpha}E_t \quad (2)$$

$$I_{t+1} = I_t + \bar{\alpha}E_t - \left(\frac{\gamma}{\delta}\right) I_t \quad (3)$$

$$R_{t+1} = R_t + \gamma \left(\frac{1-\delta}{\delta}\right) I_t \quad (4)$$

$$D_{t+1} = D_t + \gamma I_t \quad (5)$$

Here, $t \in \{0, 1, \dots\}$ denotes the model time, and the length of a period is one day. With $(S_t, E_t, I_t, R_t, D_t)$ denoting fractions relative to population $\bar{N} > 0$, we also have

$$S_t + E_t + I_t + R_t + D_t = 1 \quad (6)$$

for any day t . For simplicity, population is assumed to be fixed in the course of disease progression.

The model can be understood in the following way: When a susceptible individual and an infectious one get in contact, there is a strictly positive probability that the susceptible individual becomes exposed to the virus. The social distancing term $d_t \in [0,1]$ in (1) and (2) determines the effective transmission rate of the disease from infectious to susceptible individuals given (S_t, I_t) and $(\bar{\beta}, \zeta)$. Here, $\bar{\beta} \in (0,1)$ is the disease-specific pure transmission probability, and ζ is a country-specific parameter that we define and discuss below. The main postulate here is that, since there is always a positive probability of infection, a particular fraction of susceptible individuals moves to the exposed compartment on any day.

The movement out of the exposed compartment is governed by the incubation period. Individuals in the exposed compartment are infected but not infectious yet. After the incubation period ends for an exposed individual, he or she moves to the infectious compartment. The disease-specific structural parameter $\bar{\alpha}$ approximates the fraction of those moving from E_t to I_t , and it is equal to the inverse of the average incubation period of the virus measured in days. Clearly, when the average incubation period is shorter, individuals in compartment E_t migrate to compartment I_t at a faster pace.

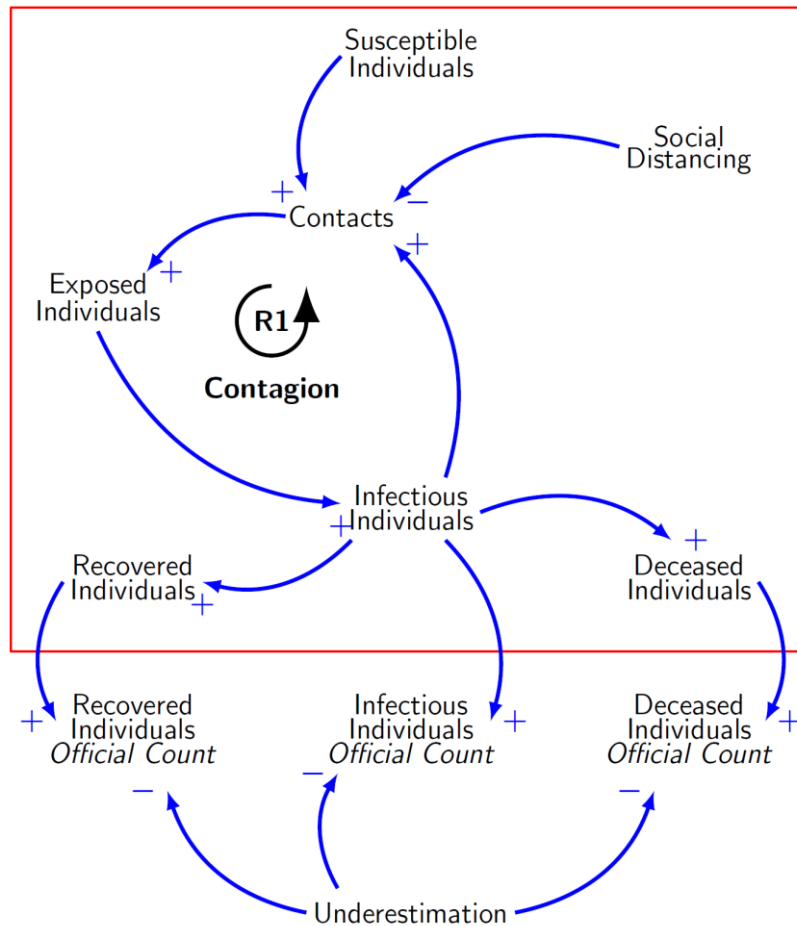
If a society achieves perfect social distancing, i.e., $d_t = 1$, then no susceptible individual gets into contact with an infectious individual, and S_t does not change. When social distancing is not perfect, i.e., $d_t < 1$, then the growth rate of E_t increases with the exposure term $(1 - d_t)$.⁵ That is, lower levels of d_t imply faster transmission of the susceptible individuals into the exposed compartment.

The pace of transmission is also affected by $\zeta > 0$. This is a country-specific and fixed parameter that we calibrate using actual data targets. The introduction of this parameter is necessary since the social distancing term d_t enters the model in an *ad hoc* way, and ζ disciplines how a particular social distancing level affects the transmission probability.⁶

⁵ The effect of social distancing on the progression of the disease is quadratic, i.e., $(1 - d_t)^2$, since social distancing is assumed to be practiced symmetrically both by susceptible and by infectious individuals.

⁶ Notice that $\bar{\beta} \in (0,1)$ and $\zeta > 0$ cannot be separately identified. For our benchmark results, we use a fixed value of $\bar{\beta}$ estimated by He, Tang, and Rong (2020). Results would remain exactly the same if we treated $\bar{\beta}\zeta$ as a single parameter.

Figure 1. Causal Loop Diagram of the SEIRD Model



The movement from the transitory compartment I_t to the terminal compartments R_t and D_t depends on two country-specific structural parameters, $\gamma \in (0,1)$ and $\delta \in (0,1)$. The former approximates the fraction of infectious individuals moving to the deceased compartment, and the latter is approximately the fraction of those dying *among the resolving cases* on a day. That is, if we denote the fraction of population in the resolving compartment on day t by Z_t , then δZ_t is the fraction of population dying on day t , and $(1 - \delta)Z_t$ is the fraction of recovering population. Here, it is important to note that I_t includes those cases that resolve on day t ; we do not model the resolving compartment separately as in Fernàndez-Villaverde and Jones (2020). As a result, the fraction of infectious individuals moving from I_t to R_t also depends on (γ, δ) . On any day, then, the movement out of I_t must be equal to the total movement into R_t and D_t .

Finally, we define the number of cumulative cases, denoted by C_t , as the total number of all currently or previously infected individuals:

$$C_t = I_t + R_t + D_t. \quad (7)$$

Figure 1 pictures the causal loop diagram of our simple model. The actual dynamics of the COVID-19 pandemic are framed within the red rectangle, and underestimation enters the model as an exogenous driving force that determines official counts of infectious, recovered, and deceased individuals.

4. Analysis

4.1. The Second Wave of the Pandemic in Türkiye

We use the SEIRD model to study the second wave of the pandemic in Türkiye. Here, the second wave refers to the period during which the daily numbers of cases started increasing again as a result of the relaxation of NPIs in June 2020. The first task is thus to determine when the second wave of the pandemic really started.

The daily increase ΔI_t in the number of individuals in the infectious compartment is a useful indicator to determine the onset of the second wave. However, since the official statistics in Türkiye do not include all confirmed cases (but reporting those with COVID-19 symptoms only) before November 25th, we have analyzed the movement of excess deaths as well.

From mid-April to the beginning of June, there has been a secular decrease in the official figures for daily COVID-19 deaths. The same pattern is observed for excess deaths, and these patterns are consistent with strict social distancing restrictions sustained in April and May.

Sometime in June and as a result of relaxed social distancing practices, we expect to observe an increase in daily COVID-19 deaths. The movement of excess deaths indicates that daily COVID-19 deaths started increasing on the last few days of May. Besides, this upward trend continued until the second week of June. Hence, it is highly probable that the second wave started right after the relaxation of NPIs in the beginning of June.

We compute ΔI_t^{off} from the official $(C_t^{\text{off}}, R_t^{\text{off}}, D_t^{\text{off}})$ figures using (4). Inspecting its movement shows that its sign is negative for all days from April 23rd to June 12th with just two exceptions (May 23rd and June 3rd). This recovery is consistent with social distancing restrictions sustained until June. Then, on June 12th, the sign is positive for *five successive days*. Such an increase almost perfectly overlaps with the timing of relaxed social distancing practices. Given the problems of data reliability for the period under consideration, the most plausible date for the onset of the second wave is thus June 12th, 2020. In fact, since the increasing trend starting on this date seems to be directly associated with the June 1st

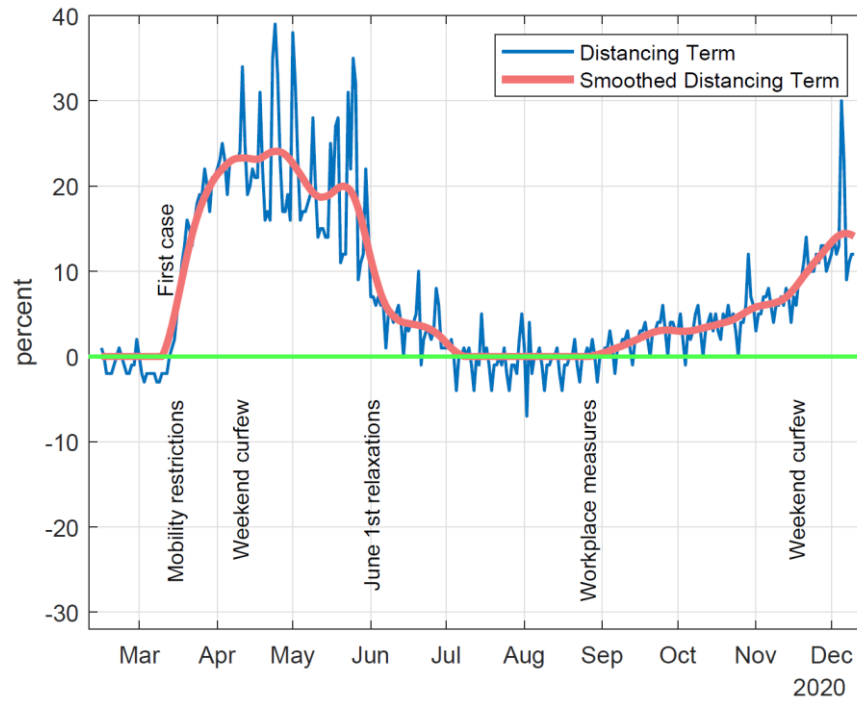
relaxations, it is reasonable to assume that the government would have been reluctant to disclose the actual number of all daily COVID-19 cases.

4.2. Epidemiological Data and Social Distancing Measures

The online repository of the *Center for Systems Science and Engineering* at Johns Hopkins University is our main source of official statistics (JHU, 2021). This repository covers daily cumulative numbers of confirmed cases (C_t^{off}) as well as recovered (R_t^{off}) and deceased (D_t^{off}) individuals. Clearly, these official statistics are not reliable especially for the second wave of the pandemic in Türkiye. Hence, our objective is to estimate *actual*, daily totals of C_t and D_t for the second wave using the SEIRD model. The official statistics are used for comparison purposes and only for the post-June 12 period.

To simulate the model, we also need a proxy for the social distancing measure d_t . Daily mobility statistics published by Apple (2021) and Google (2021) are potentially useful in this respect since it is possible to derive a social distancing measure in percentage terms using such mobility statistics. However, there are various mobility indicators in each of these sources, and their methods of benchmarking for the pre-pandemic era also differ. It turns out that Google's mobility measure for the residential areas is the most representative one since residential mobility is directly related with lockdown policies that limit mobility in public spaces. Besides, Google (2021) uses a larger time interval to normalize the pre-pandemic levels of mobility.

To derive the social distancing proxy d_t using the raw *mobility* data from Google (2021), we employ the following steps: First, we interpret increased mobility in residential areas directly as increased social distancing in public spaces. Since the raw data is already expressed in percentage increases relative to the pre-pandemic benchmark, dividing it by 100 gives us a non-smoothed measure of d_t that lies in the $[0,1]$ interval.

Figure 2. Social Distancing in Türkiye during the COVID-19 Pandemic

Notes: The raw data on residential mobility is obtained from Google (2021).

In the second step, this sequence is smoothed via the Gaussian smoothing method as in Attar and Tekin-Koru (2022). Here, smoothing is necessary for two reasons: First, we are working with a deterministic version of the SEIRD model, and our main purpose is to generate interval estimates for cases and deaths; we do not aim to explain daily fluctuations. Second, the social distancing term obtained from Google is negative (but very close to zero) on certain days. These days are the ones where mobility is slightly lower relative to the benchmark period. However, in the model, these days should correspond to $d_t = 0$ since it is the theoretical lower bound. Here, the Gaussian smoothing achieves exactly what we need; smoothed d_t is equal to zero if the nonsmoothed data point is sufficiently close to zero. Figure 2 shows the social distancing patterns in Türkiye during the COVID-19 pandemic.

4.3. Identification and Calibration

The purpose of our quantitative algorithm is to identify and calibrate the country-specific parameters (ζ, γ, δ) given the fixed values of disease-specific parameters $(\bar{\beta}, \bar{\alpha})$.

Identification of structural parameters in a SEIRD model using epidemiological data is not a straightforward task (Avery, Bossert, Clark, Ellison, & Ellison, 2020; Korolev, 2021).

A SEIRD model may yield observationally-equivalent epidemiological outcomes for widely differing parameter values. Besides, without explicit analytical solutions, identification is necessarily computational.

Our identification strategy uses two data moments to identify two parameters, and we infer from our numerical work that identification is exact; one of the parameters is more sensitive to one of these data moments, and the other parameter is more sensitive to the other data moment (see below).

Specifically, our strategy is centered around the simulation of the SEIRD model through forward recursions and builds on the following information on the actual dynamics of the COVID-19 pandemic (in Türkiye):

- Verity et al. (2020) show that COVID-19 has a particular range of *Infection Fatality Ratio* (IFR), defined as the ratio of the total number of deceased individuals to the total number of cases: $IFR_t = D_t/C_t$. Their estimates suggest a lower bound of 0.39%, an upper bound of 1.33%, and a mean value of 0.66%. We take these IFR levels as disease-specific parameters that must be satisfied in any country.
- While we do not observe the actual number of cases in Türkiye before November 25th, 2020 because of the data disclosure practices of the government, we have a particularly useful information for a specific date. Using the information revealed by the *Minister of Health* of Türkiye during a press interview, Uçar, Arslan, and Balcı Yapalak (2020, November 23) infer that the ratio of daily new *cases* to daily new *patients*, denoted here by CP_t , was equal to 6.87 on October 3rd, 2020.

The main problem of identification we face here is the following: We presume that official statistics are not reliable for the period after June 12th, 2020. Hence, we do not have any other data moments that are sufficiently informative for the unique identification of δ and γ for Türkiye. Consequently, we need to fix either δ or γ at the outset.

It seems reasonable to fix the death rate δ since its interpretation is clearer compared to γ 's—recall that δ is the daily fraction of deaths among all resolving cases on a particular day. With a fixed value of δ (and with various runs that use different δ values between 1% and 5%), we can use the two data moments described above to identify ζ and γ .

How are the two data moments informative for the two country-specific structural parameters? Evidently, both ζ and γ affect the dynamics of the disease progression in complicated ways because of the very nature of the SEIRD model. However, our numerical investigations show that, given δ , the IFR targets are relatively more informative for γ , and the case-patient ratio CP is relatively more informative for ζ . Hence, we believe that these two targets *jointly* and *exactly* identify the unknown country-specific parameters.

A computationally costless way of inferring ζ and γ is to minimize a quadratic form that represents the distance between model moments and data moments. Specifically, for a given level of δ , we minimize the following quadratic form by choosing ζ and γ :

$$Q(\zeta, \gamma) = [\text{IFR}_T^{\text{data}} - \text{IFR}_T^{\text{model}}(\zeta, \gamma)]^2 + [\text{CP}_\tau^{\text{data}} - \text{CP}_\tau^{\text{model}}(\zeta, \gamma)]^2 \quad (8)$$

Here, T refers to the end date of our sample, i.e., December 10th, 2020, and τ refers to October 3rd, 2020 for which we know the (approximate) case-patient ratio. In practice, we use the three values of $\text{IFR}_T^{\text{data}}$ and seven different values of the death rate δ . Hence, we run the calibration algorithm 21 times to obtain 21 different pairs of (ζ, γ) for Türkiye.⁷

Needless to say, the algorithm is supplied with the “initial” values $(S_0, E_0, I_0, R_0, D_0)$ for June 12th, 2020 that corresponds to the first day in the model, i.e., $t = 0$. These values and the benchmark levels of $(\bar{\beta}, \bar{\alpha})$ are borrowed from Attar and Tekin-Koru (2022). The pure transmission probability $\bar{\beta}$ is equal to 0.111 as estimated by He et al. (2020), and the average incubation period, denoted by $1/\bar{\alpha}$, is set to 7 days as it is typical in the related literature (Tang et al., 2020). Finally, for simplicity, we set the total population of Türkiye to 83,429,607, i.e., the official population of the country in the year 2019. Table 1 collects the model inputs utilized by the calibration algorithm. The initial date corresponds to $t = 0$ in the model and to June 12th, 2020 in the data. Table 2 documents the results of three runs of the calibration algorithm for the death rate $\delta = 4\%$. In all of these runs, the algorithm minimizes $Q(\zeta, \gamma)$ by choosing (ζ, γ) where $\text{CP}_\tau^{\text{data}}$ is set to 6.87. We start with the same initial guesses for (ζ, γ) and use a simple routine of local optimization. Clearly, both targets are achieved with considerable accuracy, and the objective function $Q(\zeta, \gamma)$ remains very close to zero in all three of the executions.⁸

The parameter ζ , determining the effective rate of transmission given the pure transmission probability $\bar{\beta} = 0.111$, is lower than unity. This means that, given $(1 - d_t)^2$ and depending on the magnitude of d_t , the calibration targets revise the transmission probability down to a lower level.

⁷ Since we have only two moments (m_1, m_2) for two parameters, we do not attempt a two-step or continuously-updated estimation of optimal weights for these two moments. Besides, in all of the 21 specifications, we observe that the relative deviation $(m_1^{\text{model}}/m_1^{\text{data}})/(m_2^{\text{model}}/m_2^{\text{data}})$ is close to unity, implying that optimal weights may not yield considerable gains. Another related issue is whether we should have defined the quadratic form via scaled differences $(m^{\text{model}} - m^{\text{data}})/m^{\text{data}}$. While rescaling is generally preferable, our results are not sensitive in this respect.

⁸ Please see Appendix A for detailed calibration results of all 21 specifications and for technical details about the numerical optimization routine we use.

Table 1. Calibration Inputs

	Values	Sources
<i>Disease-specific parameters</i>		
$\bar{\beta}$	0.111	He et al. (2020)
$\bar{\alpha}$	1/7	Tang et al. (2020)
<i>Initial values</i>		
S_0	0.99781158	
E_0	0.00008823	
I_0	0.00025576	Attar & Tekin-Koru (2022)
R_0	0.00178716	
D_0	0.00005727	
<i>Population</i>		
\bar{N}	83,429,607	UNPF (2021)
<i>Alternative IFR targets</i>		
	0.39%	
IFR_T^{data}	0.66%	Verity et al. (2020)
	1.33%	
<i>Alternative death rates</i>		
δ	{1.0%, 1.2%, 1.5%, 2.0%, 3.0%, 4.0%, 5.0%}	

Table 2. Calibration Results for $\delta = 4\%$ and $CP_\tau^{data} = 6.87$

	$IFR_T^{data} = 0.66\%$	$IFR_T^{data} = 0.39\%$	$IFR_T^{data} = 1.33\%$
ζ	0.30544199	0.29011661	0.35406967
γ	0.00012012	0.00004386	0.00035678
CP_τ^{model}	6.86997594	6.86998216	6.87001287
IFR_T^{model}	0.65945713	0.38955008	1.32998076
$Q(\zeta, \gamma)$	0.00000030	0.00000020	0.00000000
C_T^{model}	2,133,948	2,160,373	2,062,951
C_T^{data}	1,748,567		
D_T^{model}	14,072	8,416	27,437
D_T^{data}	15,751		
T	Dec. 10, 2020		
τ	Oct. 3, 2020		

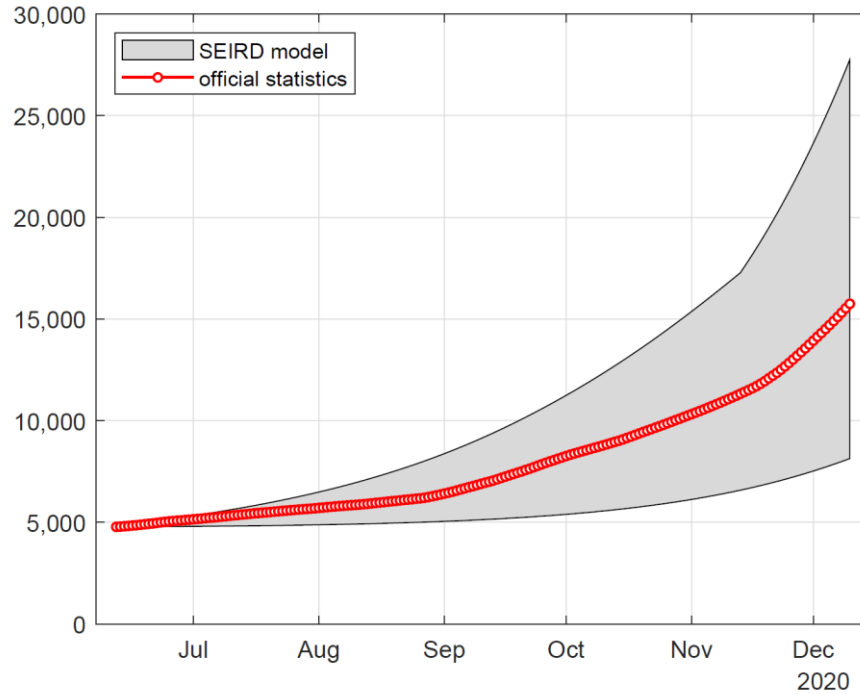
The parameter γ determines the fraction γ/δ of individuals leaving the infectious compartment on each day for any given level of δ . The algorithm returns very low levels for γ in all of the runs. However, we also observe sizable differences for changing IFR targets. For $\delta = 4\%$ and the upper bound IFR target of 1.33%, we have $\gamma/\delta = 0.0089$, implying that, on any given day, roughly 0.9% of individuals in the infectious compartment leave for the recovered and deceased compartments. For the lower bound IFR target of 0.39%, this rate is equal to $\gamma/\delta = 0.0011$. That is, roughly 0.1% of infectious individuals become recovered or deceased on a daily basis. Without actual data on the fraction I_t of individuals in the infectious compartment, it is not possible to find a useful benchmark for comparison. But the model at least allows us to differentiate the individuals moving into compartment R_t from those moving into compartment D_t . Recalling that compartment I_t in our setup includes the resolving cases on day t , the parameter γ gives the fraction of infectious individuals that die on a day.

5. Results

We present the main results of our paper in this section. For both cases and deaths as well as IFR, we provide intervals for each day in our sample. Recall that we have 21 different specifications of $(\delta, \text{IFR}_T^{\text{data}})$ for the determination of (ζ, γ) , and our interval estimations give the maximum-minimum bounds for each day in our sample across all 21 specifications. We also run two counterfactual experiments to investigate the role of social distancing for epidemiological outcomes.

5.1. COVID-19 Deaths and Cases in Türkiye

After obtaining the simulated data for each of the 21 specifications, we compute the minimums and maximums of cumulative deaths (D_t) and cases (C_t) for each day across different specifications (Figures 3 and 4, respectively). Consequently, for both cases and deaths, we derive the SEIRD model bounds for each day in our sample that runs from June 12th to December 10th. Additionally, we document the SEIRD model bounds for IFR and compare them with the official IFR statistic for each day (Figure 5).

Figure 3. Cumulative COVID-19 Deaths in Türkiye

Notes: This figure shows the estimated SEIRD model bounds (grey area) and the official figure (red circles) for cumulative COVID-19 deaths.

In Figures 3, 4 and 5, the reader would notice that official statistics may or may not remain within the SEIRD model bounds for any given day. The model bounds for cumulative deaths, for instance, include the official statistic for almost the entire sample period, most definitely after mid-July. However, for cumulative cases and for IFR, official statistics are generally not included within the model bounds. They return to the model bounds only when they are disclosed truthfully at the very end of our sample, on December 10th. When the official statistic for any given day is lower than the lower bound (*or* higher than the upper bound) implied by one of the 21 runs of the SEIRD model, this identifies that the epidemiological variable in question is underestimated (*or* overestimated). In this case, the extent of underestimation (*or* overestimation) is at least the difference between the lower model bound and the official figure (*or* between the official figure and the upper model bound). When the official statistic for any given day is within the model bounds, however, the lower bound of the model is not a useful point of reference for underestimation. In such a case, the extent of underestimation should be evaluated by inspecting the difference between the upper bound implied by the model and the official figure.

Deaths. Figure 3 pictures the model-based results for cumulative deaths. The gray area is the interval we derive using the SEIRD model. The red line with circle markers is the official death total.

Figure 3 shows that the vertical distance between the upper bound of the SEIRD model and the official figures continues to grow after late July. If we take the official COVID-19 deaths as the most plausible minimum and the upper bound of the SEIRD model as the most plausible maximum, the difference on the last day of our sample is slightly less than 13,000 deaths. Clearly, the lower bound we estimate is not informative *ex post* since the official death count is larger than this minimum for all days in the sample.

Figure 3 also shows that, compared with the earlier period, both the upper bound we estimate and the official death total increase at faster rates after mid-November. This acceleration is observed despite the weekend curfews and some other mobility restrictions reinstated on November 17th. However, the increasing pace of death totals is due to the delayed effect of *no social distancing* continued until the end of August and *loose social distancing* observed in September and October.

In short, the evolution of COVID-19 deaths originating from the SEIRD model indicates that official COVID-19 statistics in Türkiye underestimate the actual death toll during the second wave of the pandemic.⁹

Cases. We present the simulation results for cumulative cases in Figure 4. Once again, the gray area represents the SEIRD model bounds, and the red line with circle markers is the official case count.

The most significant outcomes are (i) the wide gap between the model bounds and the official figure, and (ii) the jump on December 10th that eventually locates the total number of cases within the model bounds.¹⁰

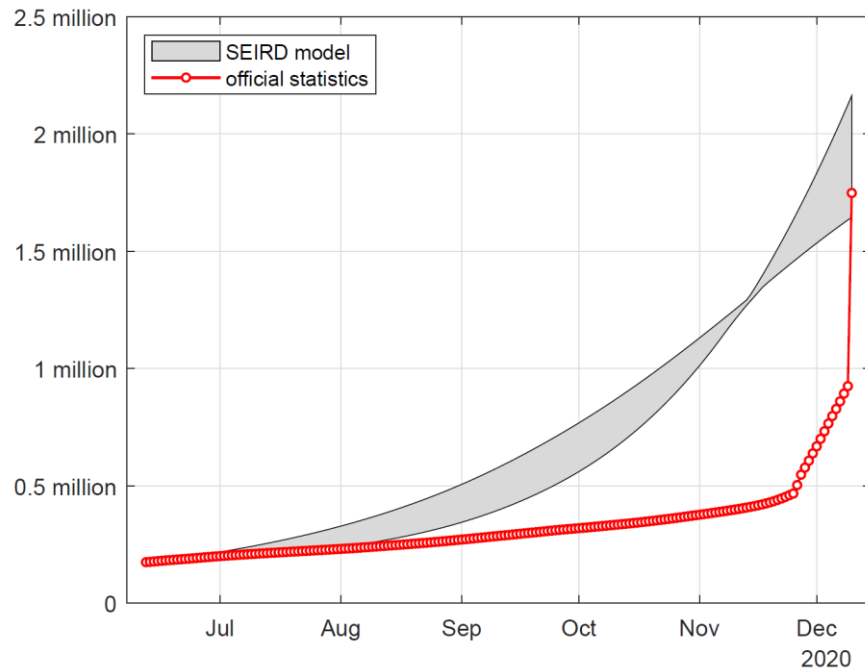
Figure 4 shows that there is a large and growing difference between the upper bound originating from the SEIRD model and the official case count. The difference is more visible after mid-July and is around 250,000 cases in the beginning of September. At the end of September, the difference reaches a level slightly less than 500,000 cases, and it is over 750,000 cases at the end of October. These dynamics are not surprising since the government

⁹ The multiplication factor that is equal to unity on June 12th by construction persistently increases to a level slightly less than two at the end of our sample period.

¹⁰ Cumulative case counts originating from our SEIRD model runs are all close to 1.3 million in mid-November. Hence, the SEIRD model bounds seem to be converging to each other in a particular week. While a mathematical proof of why this must be the case is not feasible, we explain why this is a typical feature of a SEIRD model in Appendix B.

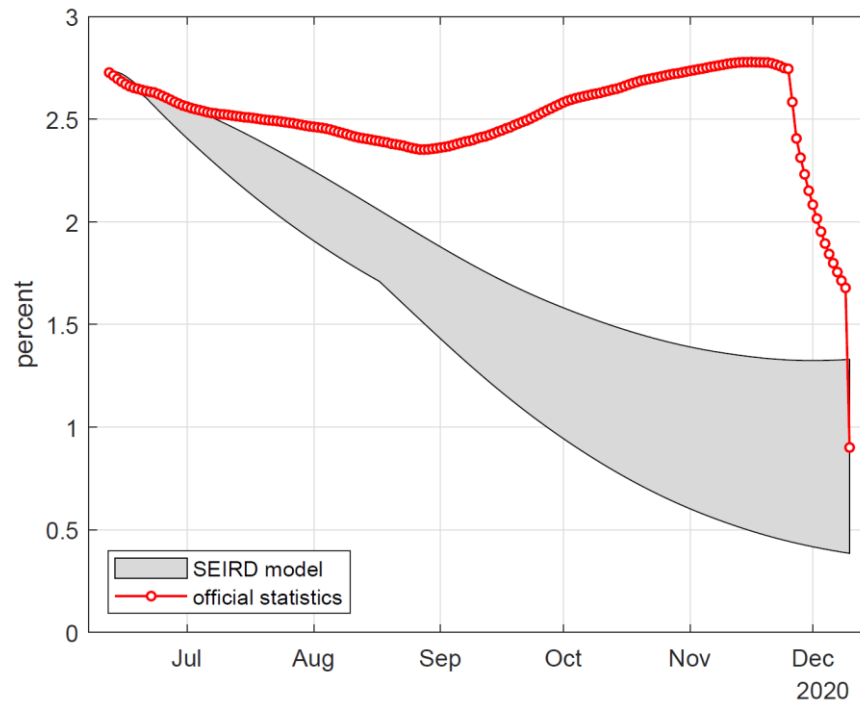
was announcing only the patients with symptoms, at least after the end of July, and we do not even know what fraction of all cases in the country could have actually been confirmed.

Figure 4. Cumulative COVID-19 Cases in Türkiye



Notes: This figure shows the estimated SEIRD model bounds (gray area) and the official figure (red circles) for cumulative COVID-19 cases.

On the day the government starts disclosing the daily cases confirmed through tests (not just the patients with symptoms), i.e., on November 25th, the difference between the upper bound and the official figure is 1,166,942 cumulative cases. Then, on December 10th, the government announces the cumulative case count (not just the cumulative patient count), and that particular official figure lies within our model bounds. This means that, if the official cumulative figure the government announced on December 10th is truthful, the SEIRD model performs remarkably well by targeting the IFR bounds for Türkiye.

Figure 5. Infection Fatality Ratio in Türkiye

Notes: Infection Fatality Ratio is defined as the ratio of total death count to total case count. The gray area pictures the estimated SEIRD model bounds for IFR, and the red circles show the official figure.

Infection Fatality Ratio. Figure 5 pictures the evolution of IFR from June 12th to December 10th where the gray area is again representing the SEIRD model bounds and the red line with circle markers the official ratio. Recall that the SEIRD model presumes that the June 12th official data is correct. The model then targets IFR_7^{model} at the end of the sample at three different levels.

The figure shows that the official ratio remains much larger than the SEIRD model maximum after the first week of July. The official ratio abruptly drops on December 10th when the Ministry of Health started reporting the total number of confirmed cases. On this day, the model bounds include the official ratio as in Figure 4.

Similar to the dynamics of cumulative cases discussed above, we learn a great deal about the strange data disclosure practices of the government from Figure 5. First, the evolution of the official IFR figure throughout the second wave has such a strange shape, and it remains well above 2% most possibly as a result of official case count being too low. Second, the official IFR figure on December 10th lies within the model bounds, and this shows that, if the government's December 10th announcement is truthful, then the version of the

SEIRD model we calibrate for the pandemic in Türkiye is exceptionally well-performing even though it only has five compartments.

5.2. Counterfactual Social Distancing Scenarios

How COVID-19 progresses in time crucially depends on the effective rate of transmission, and this effective rate depends on *de facto* social distancing practices of susceptible and infected individuals in the society (Attar & Tekin-Koru, 2022; Siedner et al., 2020).

In this subsection, we investigate the effects of two counterfactual social distancing scenarios. To this end, we feed the model with two alternative sequences of the social distancing term d_t and compare counterfactual outcomes of cases and deaths with official statistics and with the benchmark values from the SEIRD model. For both scenarios, we take the specification with $IFR_T^{\text{model}} = 1.33\%$ and $\delta = 4\%$ as the SEIRD model benchmark, and we do so for two reasons: First, the specifications with $IFR_T^{\text{model}} \in \{0.39\%, 0.66\%\}$ imply fewer deaths than the official death count. Second, among the specifications with $IFR_T^{\text{model}} = 1.33\%$, the death rate of $\delta = 4\%$ yields the highest accuracy in the sense that $Q(\zeta, \gamma)$ assumes the lowest value among all executions.

As we explain below in detail, we consider the following social distancing scenarios in our counterfactual analyses:

- A Longer Initial Lockdown Ending on July 1st
- Social Distancing Sustained at its Historical Maximum

The rationale for the former is that June 1st relaxations were implemented at a time when the daily number of new cases was at its minimum observed after the first peak. It is thus interesting to see the effects of an alternative lockdown where relaxations are delayed. What motivates the second scenario is the notion that social distancing and lockdowns should either be exercised strictly to control the epidemic as early as possible or not at all (Çakmaklı et al., 2023; Maharaj & Kleczkowski, 2012). Türkiye's case is thus informative for the effects of sustained and effective mobility restrictions.

Scenario 1: A Longer Initial Lockdown. The Turkish government adopted the first set of NPIs against COVID-19 in March 2020 after confirming the first cases of COVID-19. As noted above, these initial sets of policy measures included school and workplace closures (including restaurants, coffee shops, and night clubs), travel restrictions, and other measures such as the cancellation of public events and gatherings. However, these restrictions were relaxed significantly in the beginning of June 2020.

As our first counterfactual scenario, we consider a longer initial lockdown that ends not on June 1st but on July 1st. We chose such an alternative since official statistics indicate that the progression of COVID-19 significantly slowed down throughout the initial lockdown. This, of course, was accompanied with a severe contraction of real economic activity. The interesting question here is whether and how bearing the economic burden of the initial lockdown a little longer would alter the pandemic outcomes.

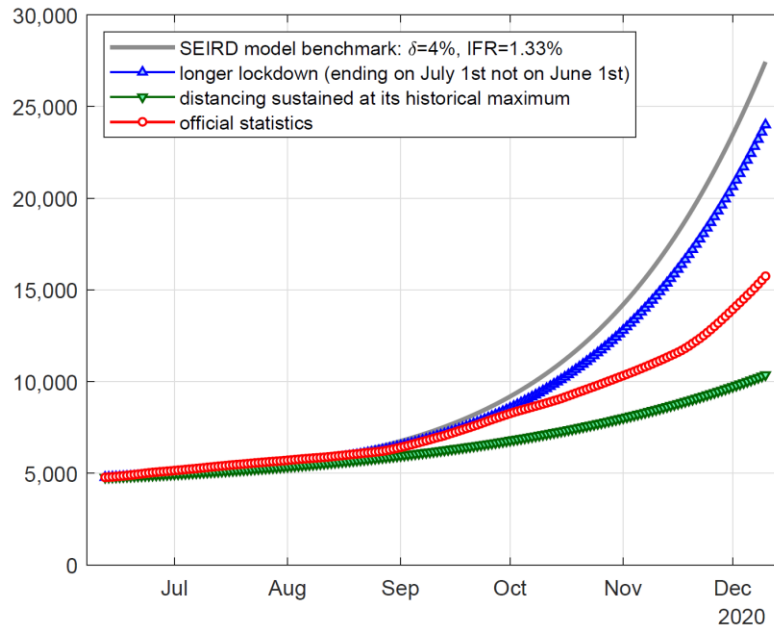
To construct the alternative d_t sequence for the first scenario, we assume that the July 1st relaxation would have the same shape and scale we observe for the June 1st relaxation.

Scenario 2: Social Distancing Sustained at its Historical Maximum. The second counterfactual scenario represents *the best practice* social distancing from the perspective of the control of disease transmission. In this scenario, we assume that society sustains social distancing at the maximum level that it achieved since the beginning of the pandemic in March 2020.

The smoothed social distancing measure we use indicates that Türkiye achieves maximum social distancing on April 24th, 2020 with $d_t = 24\%$. We thus feed the model with a constant value of 24% for the entire post-June 12th sample.

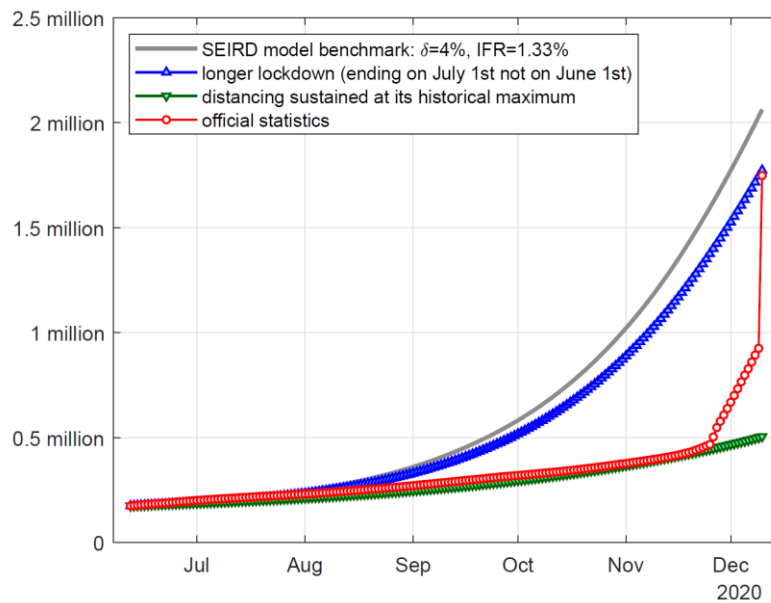
Figures 6 and 7 show the results of our counterfactual simulations for cumulative COVID-19 deaths and cases, respectively. Regarding the evolution of cumulative COVID-19 deaths, both counterfactual scenarios yield lower deaths relative to the SEIRD model benchmark as expected. A longer initial lockdown has a smaller effect on cumulative deaths; at its highest, the difference with the benchmark is around 3,000 fewer deaths on December 10th, 2020. Compared with the official figures, cumulative deaths under a longer initial lockdown diverge from the official death toll after October.

Figure 6. Counterfactual Cumulative COVID-19 Deaths in Türkiye



Notes: This figure shows the cumulative deaths for counterfactual and benchmark scenarios as well as the official figure.

Figure 7. Counterfactual Cumulative COVID-19 Cases in Türkiye



Notes: This figure shows the cumulative cases for counterfactual and benchmark scenarios as well as the official figure.

For the second scenario with social distancing sustained at its historical maximum, we observe a growing gap between the SEIRD model benchmark and the counterfactual, especially after September. On the last day of our sample—December 10th—maximum social distancing is associated with around 17,000 fewer deaths relative to the benchmark and with around 5,000 fewer deaths relative to the official death toll.

The results of our counterfactual analysis for cumulative COVID-19 cases, summarized in Figure 7, are also interesting. First, as expected after Figure 6, the effect of a longer lockdown is not pronounced relative to the benchmark. Second, maximum social distancing returns the most favorable outcomes in terms of the cumulative number of cases. Specifically, if social distancing was sustained at its historical maximum all along, then the total number of confirmed cases would be lower than the model benchmark by around 1.5 million cases on December 10th. Put differently, there is a very large and growing gap between the case totals implied by the model benchmark and those implied by maximum social distancing.

The striking feature of Figure 7 is the coincidental overlap of the official figure and the maximum social distancing scenario before November 25th. Then, on December 10th, the official figure jumps again as the total number of cases was disclosed by the Ministry of Health. On this date, again coincidentally, the official figure is very close to the case total implied by the longer lockdown scenario.

For the simulation results presented in Figure 7, we must emphasize that the overlaps are indeed coincidental; we are not aware of any model-building effort by the Ministry of Health that utilizes Google mobility data and/or investigates the effects of lockdowns that sustain social distancing at its historical maximum. If, however, the strange data disclosure practices would have been imagined to be complemented with the fabrication of epidemiological data, then an interesting and convincing way to do so would be to observe the maximum level of social distancing and run a counterfactual SEIRD model exactly as we have done in this paper!

6. Conclusion

Social scientists need efficient and effective algorithms to deal with intentional and unintentional underestimation problems. In this paper, we develop a system dynamics approach for epidemiological underestimation that works under extreme data limitations.

We construct a dynamic, nonlinear, epidemiological model designed particularly for understanding the nonmonotonic progression of an epidemic disease in time. Our main contribution to the related literature on underestimation is to identify the actual evolution of the pandemic when it is certain that official statistics are almost completely unreliable as in Türkiye. With only one observed country-specific mobility variable and only two data moments, our algorithm takes only a few minutes to identify country-specific structural parameters.

While we take the problematic second wave of COVID-19 in Türkiye as our exemplar in this paper, the algorithm can be applied, *with appropriate modifications*, to any other country, any other epidemic disease, and any wave of the COVID-19 pandemic. In the Turkish case, we use the presumably truthful revelation of actual ratio of cases to patients on October 3rd, 2020 by the Minister of Health as a useful data moment. But any reliable information on daily or cumulative deaths or cases, *even for single day*, can be used while applying our algorithm to another country or disease.

References

- Adıgüzel, F. S., Cansunar, A., & Çörekçioğlu, G. (2020). Truth or dare? detecting systematic manipulation of covid-19 statistics. *Journal of Political Institutions and Political Economy*, 1(4), 543-557.
- Apple. (2021). *Mobility trends reports*. <https://www.apple.com/covid19/mobility>.
- Attar, M. A., & Tekin-Koru, A. (2022). Latent social distancing: Identification, causes and consequences. *Economic Systems*, 46(1), 100944.
- Avery, C., Bossert, W., Clark, A. T., Ellison, G., & Ellison, S. F. (2020). Policy implications of models of the spread of coronavirus: Perspectives and opportunities for economists. *Covid Economics: Vetted and Real-Time Papers*, 1(12).
- Balashov, V. S., Yan, Y., & Zhu, X. (2020). *Are less developed countries more likely to manipulate data during pandemics? evidence from newcomb-benford law*. <https://ideas.repec.org/p/arx/papers/2007.14841.html>.
- Benford, F. (1938). The law of anomalous numbers. *Proceedings of the American Philosophical Society*, 78(4), 551-572.
- Çakmaklı, C., Demiralp, S., Özcan, Ş. K., Yeşiltaş, S., & Yıldırım, M. A. (2023). COVID-19 and emerging markets: A SIR model, demand shocks and capital flows. *Journal of International Economics*, 145, 103825.
- Çakmaklı, C., & Şimşek, Y. (2021). *Bridging the covid-19 data and the epidemiological model using time-varying parameter sird model*. Koç University-TÜSİAD ERF Working Paper, <https://eaf.ku.edu.tr/wp-content/uploads/2021/02/erfw2013.pdf>.
- Chudik, A., Pesaran, M. H., & Rebucci, A. (2021). *Covid-19 time-varying reproduction numbers worldwide: An empirical analysis of mandatory and voluntary social distancing* (Tech. Rep.). National Bureau of Economic Research.
- Degue, K. H., & Le Ny, J. (2018). An interval observer for discrete-time seir epidemic models. In *2018 annual american control conference (acc)* (p. 5934-5939).
- Dougherty, B. P., Smith, B. A., Carson, C. A., & Ogden, N. H. (2021). Exploring the percentage of covid-19 cases reported in the community in canada and associated case fatality ratios. *Infectious Disease Modelling*, 6, 123-132. Retrieved from <https://www.sciencedirect.com/science/article/pii/S2468042720301044>
- Fernández-Villaverde, J., & Jones, C. I. (2020). *Estimating and simulating a sird model of covid-19 for many countries, states, and cities* (Tech. Rep.). National Bureau of Economic Research.
- Ghaffarzadegan, N., & Rahmandad, H. (2020). Simulation-based estimation of the early spread of covid-19 in iran: actual versus confirmed cases. *System Dynamics Review*, 36(1), 101-129.

- Gibbons, C., Mangen, M., Plass, D., Havelaar, A., Brooke, R., Kramarz, P., ... Kretzschmar, M. (2014). Measuring underreporting and under-ascertainment in infectious disease datasets: a comparison of methods. *BMC Public Health*, *14*(1), 147–164. Retrieved from <https://doi.org/10.1038/s41591-020-0883-7>
- Giordano, G., Blanchini, F., Bruno, R., Colaneri, P., Filippo, A. D., Matteo, A. D., & Colaneri, M. (2020). Modelling the covid-19 epidemic and implementation of population-wide interventions in italy. *Nature Medicine*, *26*, 855–860. Retrieved from <https://doi.org/10.1038/s41591-0200883-7>
- Google. (2021). *Covid-19 community mobility results*. <https://www.google.com/covid19/mobility/>.
- He, S., Tang, S., & Rong, L. (2020). A discrete stochastic model of the covid-19 outbreak: Forecast and control. *Mathematical Biosciences and Engineering*, *17*(4), 2792-2804.
- Hellwig, C., Assenza, T., Collard, F., Dupaigne, M., Fève, P., Kankanamge, S., & Werquin, N. (2022). The Hammer and the Dance: Equilibrium and Optimal Policy during a Pandemic Crisis. *HAL Working Paper*.
- Isea, R. (2020, 06). How valid are the reported cases of people infected with covid-19 in the world? *International Journal of Coronaviruses*, *1*, 53.
- JHU. (2021). *Covid-19 data repository*. <https://github.com/CSSEGISandData/COVID-19>.
- Kaplan, G., Moll, B., & Violante, G. L. (2020). The great lockdown and the big stimulus: Tracing the pandemic possibility frontier for the US (No. w27794). *National Bureau of Economic Research*.
- Kapoor, M., Malani, A., Ravi, S., & Agrawal, A. (2020). *Authoritarian governments appear to manipulate covid data*. *Working Paper*, <https://arxiv.org/pdf/2007.09566>.
- Karlinsky, A., & Kobak, D. (2021). The world mortality dataset: Tracking excess mortality across countries during the covid-19 pandemic. *medRxiv*. Retrieved from <https://www.medrxiv.org/content/early/2021/04/11/2021.01.27.21250604>
- Kermack, W. O., & McKendrick, A. G. (1927). A contribution to the mathematical theory of epidemics. *Proceedings of the Royal Society of London. Series A, Containing Papers of a Mathematical and Physical Character*, *115*(772), 700–721.
- Korolev, I. (2021). Identification and estimation of the seird epidemic model for covid-19. *Journal of Econometrics*, *220*(1), 63-85.
- Krantz, S. G., & Srinivasa Rao, A. S. R. (2020). Level of underreporting including underdiagnosis before the first peak of covid-19 in various countries: Preliminary retrospective results based on wavelets and deterministic modeling. *Infection Control & Hospital Epidemiology*, *41*(7), 857-859.
- Kung, S., Doppen, M., Black, M., Braithwaite, I., Kearns, C., Weatherall, M., ... Kearns, N. (2021). Underestimation of covid-19 mortality during the pandemic. *ERJ Open Research*, *7*, 1-7.

- Maharaj, S., & Kleczkowski, A. (2012). Controlling epidemic spread by social distancing: Do it well or not at all. *BMC Public Health*, *12*(679), 1-16. Retrieved from <https://doi.org/10.1186/1471-2458-12-679>
- Millimet, D. L., & Parmeter, C. F. (2022). Covid-19 severity: A new approach to quantifying global cases and deaths. *Journal of the Royal Statistical Society: Series A (Statistics in Society)*, *185*(3), 1178–1215.
- Noufaily, A. (2019). Underreporting and reporting delays. In L. Held, N. Hens, P. O’Neill, & J. Wallinga (Eds.), *Handbook of infectious disease data analysis* (pp. 437–454). London: Chapman and Hall/CRC.
- Rahmandad, H., Lim, T. Y., & Sterman, J. (2021). Behavioral dynamics of covid-19: estimating underreporting, multiple waves, and adherence fatigue across 92 nations. *System Dynamics Review*, *37*(1), 5-31.
- Sawano, T., Kotera, Y., Ozaki, A., Murayama, A., Tanimoto, T., Sah, R., & Wang, J. (2020, 06). Underestimation of covid-19 cases in japan: an analysis of rt-pcr testing for covid-19 among 47 prefectures in japan. *QJM: An International Journal of Medicine*, *113*(8), 551-555. Retrieved from <https://doi.org/10.1093/qjmed/hcaa209>
- Siedner, M. J., Harling, G., Reynolds, Z., Gilbert, R. F., Haneuse, S., Venkataramani, A. S., & Tsai, A. C. (2020, 08). Social distancing to slow the us covid-19 epidemic: Longitudinal pretest-posttest comparison group study. *PLOS Medicine*, *17*(8), 1-12. Retrieved from <https://doi.org/10.1371/journal.pmed.1003244>
- Tang, B., Wang, X., Li, Q., Bragazzi, N. L., Tang, S., Xiao, Y., & Wu, J. (2020). Estimation of the transmission risk of the 2019-ncov and its implication for public health interventions. *Journal of Clinical Medicine*, *9*(2)(462), 1-13.
- Uçar, A., Arslan, S., & Balcı Yapalak, A. N. (2020, November 23). *Türkiye covid-19 pandemisinde resmi ve tahmini sayılar [sunum]*. *Bilim Akademisi COVID-19 Modelleme Çalıştayı*, <https://bilimakademisi.org/wp-content/uploads/2020/12/abdullah-ucar-sunum.pdf>.
- UNPF. (2021). *World population dashboard*. <https://www.unfpa.org/data/world-populationdashboard>.
- Vandoros, S. (2020). Excess mortality during the covid-19 pandemic: Early evidence from england and wales. *Social Science & Medicine*, *258*, 113101. Retrieved from <https://www.sciencedirect.com/science/article/pii/S0277953620303208>
- Verity, R., Okell, L. C., Dorigatti, I., Winskill, P., Whittaker, C., Imai, N., ... Ferguson, N. M. (2020). Estimates of the severity of coronavirus disease 2019: a model-based analysis. *The Lancet Infectious Diseases*, *20*, 669-677.
- Wu, S. L., Mertens, A. N., Crider, Y. S., Nguyen, A., Pokpongkiat, N. N., Djajadi, S., ... Benjamin-Chung, J. (2020). Substantial underestimation of sars-cov-2 infection in the united states. *Nature Communications*, *11*(4507), 1-10. Retrieved from <https://doi.org/10.1038/s41467-020-182724>

DISCLOSURE STATEMENTS:**Research and Publication Ethics Statement:**

This study has been prepared in accordance with the rules of scientific research and publication ethics.

Contribution Rates of the Authors:

The first author's contribution is 50%, and the second author's is 50%.

Conflicts of Interest:

On behalf of all authors, the corresponding author states that there is no conflict of interest.

Financial research support statement and acknowledgement:

This study was not supported by an organization. We thank the editor Fatma Dođruel and two anonymous reviewers for their helpful comments and suggestions on an earlier version. We also thank Zeki Berk, Mehmet Somel, Abdullah Uçar, and Güçlü Yaman who have generously shared with us their estimated and/or compiled COVID-19 data on cases and (excess) deaths in Türkiye. Finally, we also wish to thank many conference and seminar participants who have provided helpful comments and suggestions on earlier versions of this paper. All of the remaining errors are ours.

Ethics Committee Approval:

Ethics committee approval was not obtained because human subjects were not used in the research described in the paper.

Supplementary Materials:

The computer programs written in MATLAB and the original data files for this article are publicly available at <https://github.com/maattar/Epidemiological-Underestimation.git>

Appendices

Appendix A: Calibration Results

The seven tables presented below collect the detailed calibration results for seven different values of δ , i.e., the fixed death rate among the resolving cases. The algorithm minimizes the quadratic form $Q(\zeta, \gamma)$ by choosing (ζ, γ) from a compact set where $\zeta \in [0, 2]$ and $\gamma \in [0, 0.005]$. For all the runs, the initial guesses are $\zeta = 0.4$ and $\gamma = 0.001$.

The tables below have three columns documenting the results, and each column corresponds to a particular run of the calibration algorithm with a given IFR target for December 10th, 2020: $\text{IFR}_T^{\text{data}} \in \{0.39\%, 0.66\%, 1.33\%\}$. The other data moment that is common across all specifications is the case-patient ratio $\text{CP}_\tau^{\text{data}}$ on October 3rd, 2020 and is set to 6.87 (Uçar et al., 2020).

The algorithm uses MATLAB’s “fmincon” routine. By default, this routine searches for an interior optimum within a compact set. The Hessian is approximated through the Broyden–Fletcher–Goldfarb–Shanno algorithm. In all of the runs, the algorithm has converged to a solution by hitting the step-size tolerance that is equal to 10^{-20} .

Table A.1: Calibration Results for $\delta = 1\%$

	$\text{IFR}_T^{\text{data}} = 0.66\%$	$\text{IFR}_T^{\text{data}} = 0.39\%$	$\text{IFR}_T^{\text{data}} = 1.33\%$
ζ	0.41311650	0.31833305	1.79925404
γ	0.00015896	0.00004590	0.00163752
$\text{CP}_\tau^{\text{model}}$	6.86969279	6.86983096	6.86470456
$\text{IFR}_T^{\text{model}}$	0.65195260	0.38507261	1.15113794
$Q(\zeta, \gamma)$	0.00006486	0.00002431	0.03201968
C_T^{model}	1,995,980	2,113,317	1,645,057
D_T^{model}	13,013	8,138	18,937

Table A.2: Calibration Results for $\delta = 1.2\%$

	$IFR_T^{\text{data}} = 0.66\%$	$IFR_T^{\text{data}} = 0.39\%$	$IFR_T^{\text{data}} = 1.33\%$
ζ	0.38363504	0.31214880	1.62699469
γ	0.00014924	0.00004596	0.00175058
CP_{τ}^{model}	6.86984582	6.86992727	6.86965623
IFR_T^{model}	0.65610866	0.38776070	1.31213495
$Q(\zeta, \gamma)$	0.00001517	0.00000502	0.00031928
C_T^{model}	2,027,229	2,123,047	1,657,509
D_T^{model}	13,301	8,232	21,749

Table A.3: Calibration Results for $\delta = 1.5\%$

	$IFR_T^{\text{data}} = 0.66\%$	$IFR_T^{\text{data}} = 0.39\%$	$IFR_T^{\text{data}} = 1.33\%$
ζ	0.35713181	0.30584194	0.71127614
γ	0.00013930	0.00004578	0.00073892
CP_{τ}^{model}	6.86988344	6.86999244	6.86960653
IFR_T^{model}	0.65682194	0.38975343	1.31854187
$Q(\zeta, \gamma)$	0.00001011	0.00000006	0.00013144
C_T^{model}	2,058,983	2,133,294	1,812,919
D_T^{model}	13,524	8,315	23,904

Table A.4: Calibration Results for $\delta = 2\%$

	$IFR_T^{\text{data}} = 0.66\%$	$IFR_T^{\text{data}} = 0.39\%$	$IFR_T^{\text{data}} = 1.33\%$
ζ	0.33452902	0.29939993	0.49581989
γ	0.00013128	0.00004508	0.00050789
CP_{τ}^{model}	6.86997581	6.87000084	6.86983760
IFR_T^{model}	0.65905167	0.38996712	1.32581496
$Q(\zeta, \gamma)$	0.00000090	0.00000000	0.00001754
C_T^{model}	2,089,396	2,144,107	1,925,872
D_T^{model}	13,770	8,361	25,533

Table A.5: Calibration Results for $\delta = 3\%$

	$IFR_T^{\text{data}} = 0.66\%$	$IFR_T^{\text{data}} = 0.39\%$	$IFR_T^{\text{data}} = 1.33\%$
ζ	0.31453646	0.29310936	0.38985490
γ	0.00012372	0.00004412	0.00039510
CP_{τ}^{model}	6.86999531	6.86996764	6.87001764
IFR_T^{model}	0.65970339	0.38917236	1.32986580
$Q(\zeta, \gamma)$	0.00000009	0.00000069	0.00000002
C_T^{model}	2,119,290	2,155,029	2,020,368
D_T^{model}	13,981	8,387	26,868

Table A.6: Calibration Results for $\delta = 4\%$

	$IFR_T^{\text{data}} = 0.66\%$	$IFR_T^{\text{data}} = 0.39\%$	$IFR_T^{\text{data}} = 1.33\%$
ζ	0.30544199	0.29011661	0.35406967
γ	0.00012012	0.00004386	0.00035678
CP_{τ}^{model}	6.86997594	6.86998216	6.87001287
IFR_T^{model}	0.65945713	0.38955008	1.32998076
$Q(\zeta, \gamma)$	0.00000030	0.00000020	0.00000000
C_T^{model}	2,133,948	2,160,373	2,062,951
D_T^{model}	14,072	8,416	27,437

Table A.7: Calibration Results for $\delta = 5\%$

	$IFR_T^{\text{data}} = 0.66\%$	$IFR_T^{\text{data}} = 0.39\%$	$IFR_T^{\text{data}} = 1.33\%$
ζ	0.30028009	0.28833673	0.33608492
γ	0.00011816	0.00004368	0.00033762
CP_{τ}^{model}	6.86998412	6.86998724	6.87000500
IFR_T^{model}	0.65965149	0.38967514	1.33007881
$Q(\zeta, \gamma)$	0.00000012	0.00000011	0.00000001
C_T^{model}	2,142,601	2,163,593	2,087,205
D_T^{model}	14,134	8,431	27,761

Appendix B: The Evolution of Cumulative Case Count

Our purpose in this appendix is to clarify why the SEIRD model bounds seem to be converging to each other sometime in mid-November.

In the middle of November 2020, the total number C_t of confirmed cases under different specifications get extremely close to each other. There is no particular day on which such a convergence occurs, and the convergence is not absolute. Yet, on different days around November 13th, cumulative case count is close to 1.3 million people under different specifications. Since the SEIRD model is a system of nonlinear difference equations, it is not feasible to provide formal proof of this outcome. However, as shown by Li (2020), for instance, the solution of the model for C_t can be approximated by the definite solution $C_t = C_0 e^{\Theta t} + \Psi(e^{\Omega t} - e^{\Theta t})$ where $\Theta, \Psi, \Omega \in \mathbb{R}$ are meta-parameters that depend on the structural parameters of the SEIRD model, and Θ and Ω have switching signs by construction, i.e., depending on sign and magnitude restrictions on structural parameters. Furthermore, such time paths are strictly convex and strictly increasing for the beginning of a single wave of a pandemic, and the growth rate of C_t is not fixed. Hence, generally and purely from a mathematical point of view, such paths that start from the same initial value C_0 intersect once for some $t > 0$.

Our calibration algorithm chooses different (ζ, γ) pairs for different runs, and we thus obtain a particular (Θ, Ψ, Ω) tuple for each of them. Importantly, the specification that attains the lowest growth rate near $t = 0$ also attains the highest growth rate near $t = T$ and *vice versa*. With the additional restriction that the absolute increase in C_t on October 3rd ($t = \tau$) is targeted, the two paths imply similar C_t levels on a particular day between τ and T .

We should also note the following remarks regarding this feature of the SEIRD model. First, the date on which different specifications imply $C_t \approx 1.3$ million lies between τ and T since the absolute increase in C_t is targeted for τ . Second, once we change the initial values $(S_0, E_0, I_0, R_0, D_0)$ of the model in alternative runs, this particular feature vanishes. Third, the proximity of C_t to 1.3 million under different specifications is closely related with the value attained by $Q(\zeta, \gamma)$; in specifications where the algorithm is less successful in matching the targets, the SEIRD model bounds gets larger for the mid-November as well.

References for Appendices A and B

- Li, K (2020) Transmission dynamics of the global covid-19 epidemic: Analytical modeling and future prediction. *Research Square Preprint*.
- Uçar A, Arslan Ş, Balcı Yapalak AN (2020, November 23) Türkiye covid-19 pandemisinde resmi ve tahmini sayılar [sunum]. Bilim Akademisi COVID-19 Modelleme Çalıştayı.